**Year-1 Annual Report for NSF Award ATM- 0530814**

# Storm-Scale Quantitative Precipitation Forecasting Using Advanced Data Assimilation Techniques: Methods, Impacts and Sensitivities

Dr. Ming Xue[1,2], Principal Investigator
Dr. Keith Brewster[1], Co-Principal Investigator
Dr. Jidong Gao[1], Co-Principal Investigator
Dr. Alan Shapiro[1,2], Co-Principal Investigator
[1]Center for Analysis and Prediction of Storms and [2]School of Meteorology
University of Oklahoma

120 David Boren Blvd
Norman OK 73072

October 2006

Contacting e-mail: mxue@ou.edu

# 1 Introduction

Our original proposal proposed to work in the following areas: (a) Initial and boundary condition sensitivity studies and adjoint applications; (b) Initialization and prediction of convective storms using 3DVAR and complex cloud analysis and the impact and refinement of cloud analysis procedures; (c) 3DVAR analysis and assimilation of GPS slant-path integrated water vapor data and their impact on QPF; (d) Ensemble Kalman filter-based assimilation of radar and other high-resolution observations for mesoscale and storm-scale analysis and prediction; (e) 5. High-resolution simulation and analysis of convective initiation cases of IHOP_2002; (f) Sensitivity of QPF to microphysical parameterizations. Because of the reduction by about ¼ from the originally proposed budget and the removal of support for one graduate student, we stated in our impact statement that the research in areas (b) and (f) will be limited under the support of this grant, and we will not be able to work on 4DVAR data assimilation in area (a).

In spite of the reduced budget, we have been able to make significant progresses in most of the above research areas, and in some cases with leverages from other sources of support, including NSF Graduate Fellowship for one of the graduate student. Overall, the project is progressing according to and in some cases ahead of schedule. Specific achievements are summarized in the following sections.

# 2 Specific Accomplishments

## *2.1 Initial Condition Sensitivity Study Using Very Large Ensembles*

In Martin and Xue (2006a), sensitivity analyses were done using very large (several thousand member) ensembles of forward model runs that perturb the initial model fields one small patch at a time, so that sensitivity maps of the subsequent forecast fields (e.g, precipitation) to the initial condition (different variables at different regions) can be calculated. For example, sensitivity fields of the forecast precipitation to the initial low-level moisture were constructed. Some strong nonlinear sensitivity was found near the cold front. In one case, a 1 g $kg^{-1}$ perturbation at the lowest 1 km depth over a 27x27 $km^2$ area triggered an entire new storm along the cold front (Fig. 1), a sensitivity that is larger than what has been documented in the literature.

This above work has been extended more recently with new approaches that require fewer ensemble members (Martin and Xue 2006b; 2006c). In this study, a large number (~2000) of forward model runs with randomly perturbed initial fields are made and the correlation (or sensitivity) between forecast quantities and initial fields are calculated statistically. Similar methods are used in the calculation of covariances between variables at the forecast time as part of ensemble Kalman filter (EnKF) schemes which typically use 10 to 100 members. However, the calculation of sensitivities (or covariances) between a forecast quantity and model fields at an earlier time is typically much noisier than the calculation of covariances between quantities at the same time. Consequently, a much larger (than typically used) ensemble size was found to be necessary. The results thus obtained, however, are excellent, as the technique is found to accurately calculate three-dimensional initial condition sensitivity fields without the need for linearizing the model (as is required by an adjoint). The new method is much more efficient than that of the earlier method of Martin and Xue (2006a). Fig. 2 shows (a) the correlation coefficient between the total rain that fell in the indicated box, to the boundary layer water vapor field three hours earlier, and (b) the same field in a vertical cross-section.

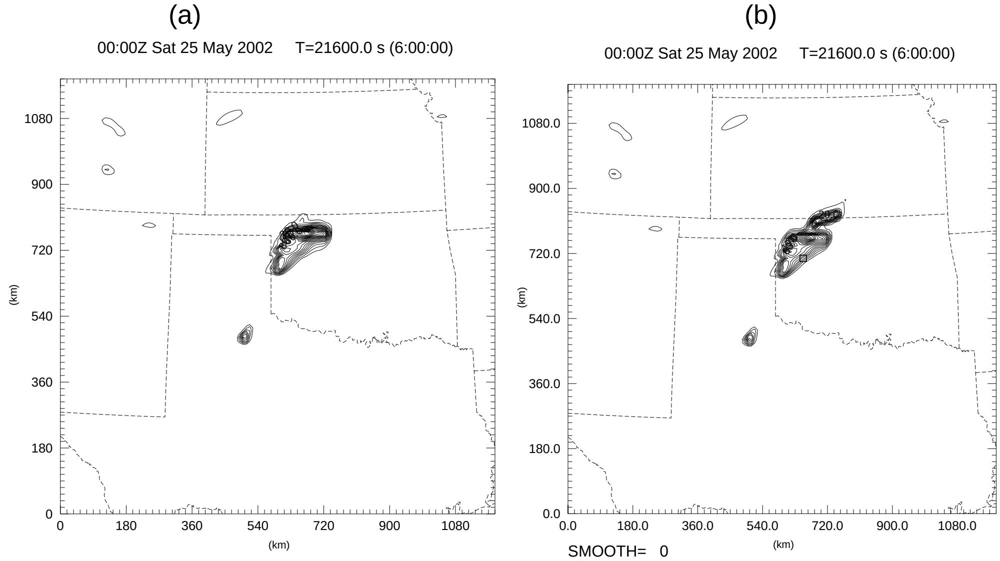


*Fig. 1. Six-hour forecast of accumulated precipitation from control run (a) and from a model run with an initial 1 g kg$^{-1}$ surface moisture perturbation at the location indicated by a small box in northwest Oklahoma (b). The extra local maximum in the precipitation along the Kansas-Oklahoma border of the perturbed run (b) is 120 mm.*

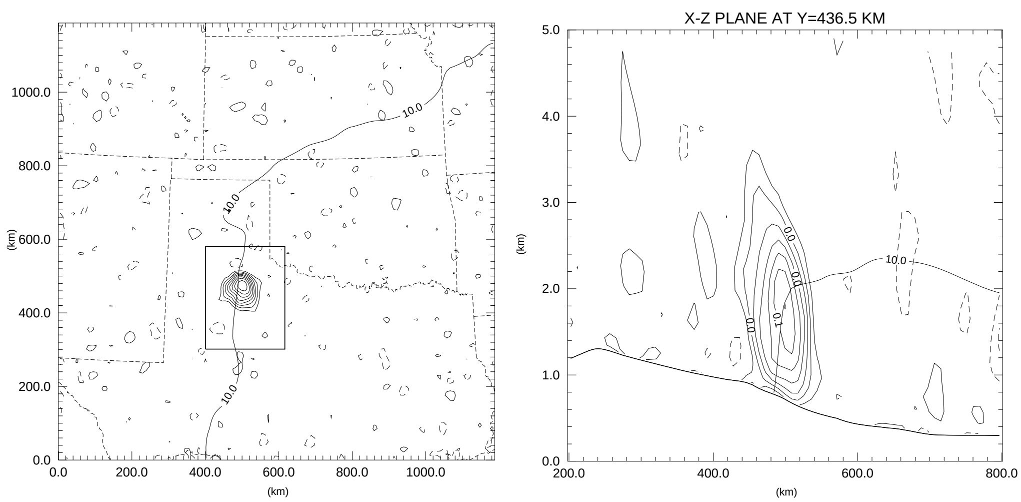


*Fig. 2. Correlation coefficient between the rain which fell in the box drawn in (left panel) to the initial boundary-layer water vapor field (left panel) and (right panel) same field but in vertical cross-section along an east-west line through the area of large correlation coefficient in the left panel.*

### 2.2 Data simulation and prediction of tornadic thunderstorms using level-II radar data with ARPS 3DVAR and cloud analysis

The ARPS 3DVAR-cloud analysis combination are shown to be efficient and effective through a number of case studies for initializing convective storms (Hu et al. 2006a; Hu et al.

2006b). Typically, rapid update cycles at 5 to 15 minutes intervals are used. Hu and Xue (2006) examined various configurations of the intermittent 3DVAR-cloud analysis data assimilation procedure for the 8 May 2003 Oklahoma City tornadic thunderstorm case, using a nested 3 km grid. Forecasts for up to 2.5 hours were made from the assimilated initial conditions. For the case, it was found that one-hour long assimilation window covering the entire initiation stage of the storm worked best. The results also show that when the data from a single Doppler radar is assimilated with properly chosen assimilation configurations, the model is able to predict the evolution of the 8 May 2003 Oklahoma City tornadic thunderstorm rather accurately for up to 2.5 hours. In Hu (2005), even better results were obtained using a 1 km grid. The prediction captured well the hook echo structure and radial velocity couplets associated with the observed tornado; they compared well against low-elevation radar observations. When a 100 m grid was further nested within the 1 km grid, an F2-intensity tornado was obtained in the model prediction (Fig. 3 and Fig. 4), whose predicted track was less than 5 km from the observed tornado track. This is, we believe, the first time ever that a tornado is predicted by a numerical model that was initialized using real data, including those of radar.

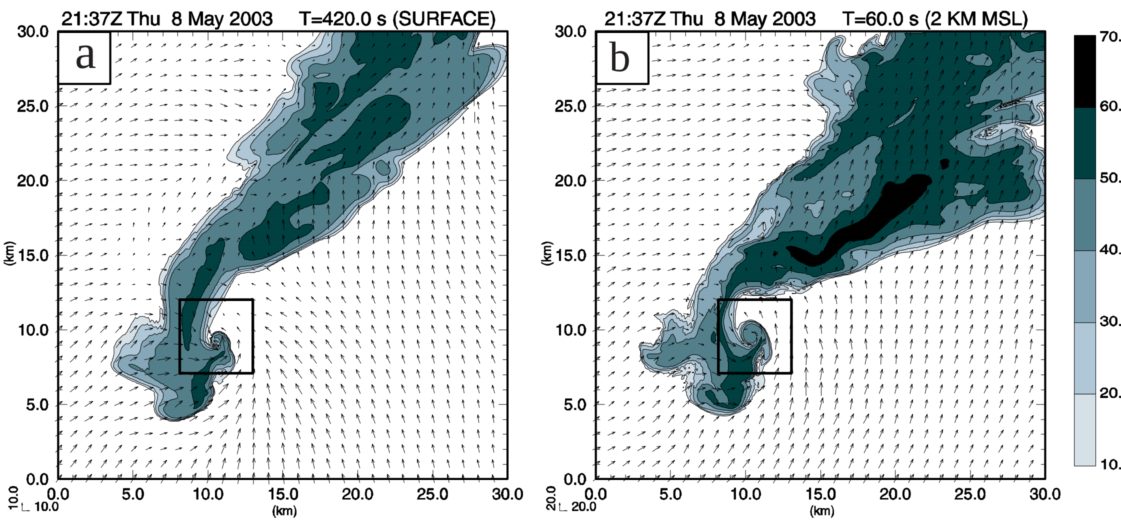


*Fig. 3 Predicted reflectivity and wind fields at the surface (left) and 2 km MSL (right) from at 7 minutes into the 100 m forecast. The square in the figures indicates a zoomed-in area to be shown in next figure. Wind vectors are plotted every 10 grid points. The presence of a tornado is indicated by the hook echo that contains reflectivity spirals into the circulation center.*

In addition, related to radar data assimilation, Gao et al. (2006c) report advances in single Doppler velocity retrieval and Gao et al. (2006a; 2006b) examine various radar ray path equations and approximations for use in radar data assimilation (DA).

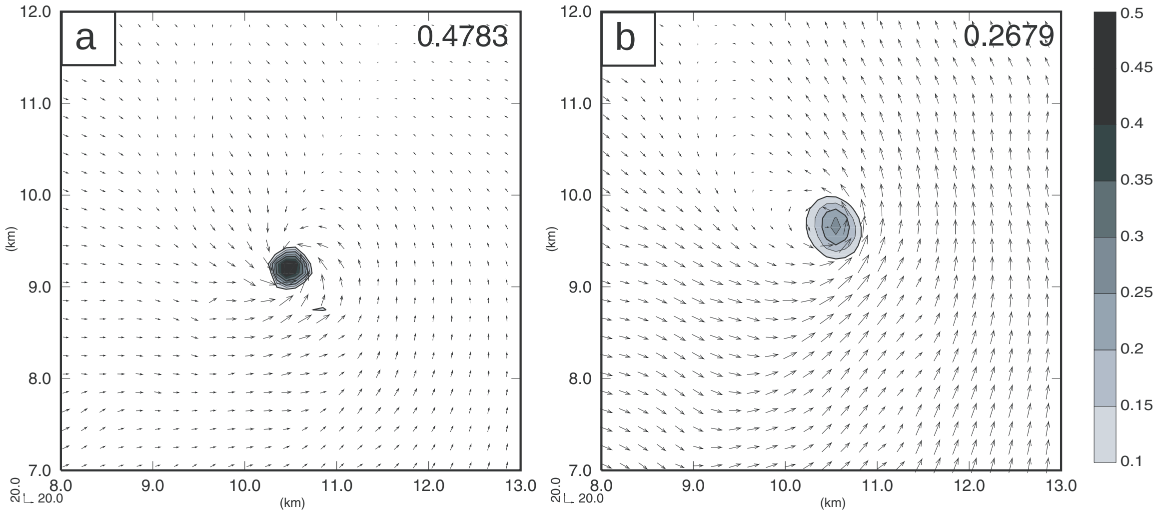


*Fig. 4. Predicted wind and vertical vorticity fields at the surface (left column) and 2 km MSL (right column) from 7 minute forecast valid at 2137 UTC. The domain corresponds to the square box found in Fig. 3. The numbers at the upper-right corner are the maximum vertical vorticity value in $s^{-1}$.*

### *2.3 3DVAR analysis of water vapor field from GPS slant-path and surface network data*

Ph.D. student, Haixia Liu developed a new univariate 3DVAR system for analyzing water vapor from GPS slant-path water vapor observations (Liu and Xue 2006a). Unique aspects of this work include the use of flow-dependent background error structures that are modeled by anisotropic explicit or recursive spatial filters. Observation system simulation experiments (OSSEs) performed for an IHOP dryline case (19 June 2002) clearly demonstrated the significant positive impact from the use of the flow-dependent background error. The analysis system was also shown, among other things, to be robust, even in the presence of observational errors and/or with a poor analysis background. The recursive filter version of the anisotropic background error has also been implemented in our 3DVAR system, improving its computational efficiency. Analyses with the recursive filter show slightly better quality than those with an explicit filter. We believe this result is due to the improved positive definiteness property of the recursive filter. The results are summarized in an accepted manuscript (Liu et al. 2006).

Fig. 5 shows results from Liu et al. (2006) comparing the moisture analyses for a dryline case from simulated slant-path water vapor data, using an isotropic recursive filter (IRF) (Fig. 5a) and a flow-dependent anisotropic recursive filter (ARF, Fig. 5b). The correlation coefficients with the truth for the analysis increments using IRF and ARF are 0.83 and 0.93, respectively, similar to the results of Liu and Xue (2006a) using explicit filters. The figure shows clearly that the anisotropic formulations outperform the isotropic ones.

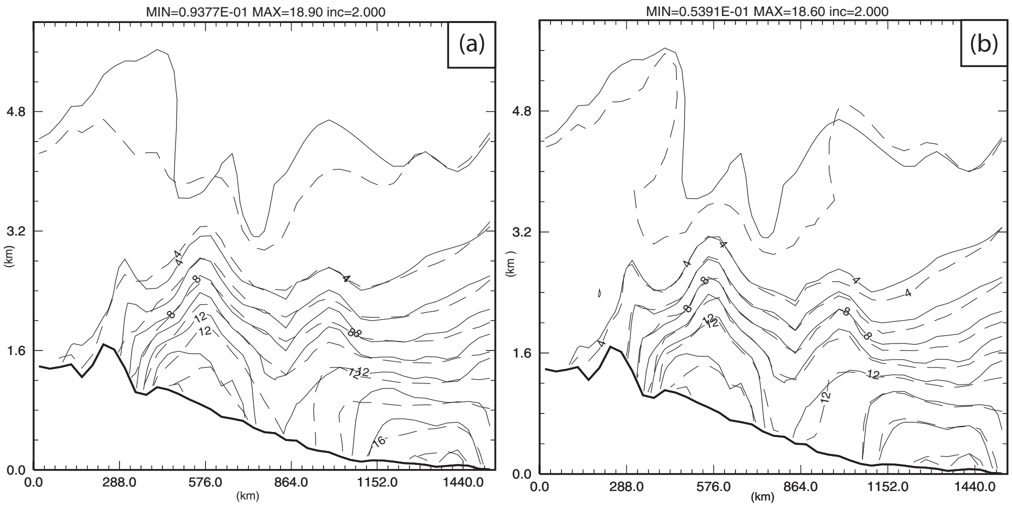


*Fig. 5. East-west cross-section of specific humidity field through a simulated dryline from IHOP_2002, as analyzed using 3DVAR (dashed lines) with (a) an isotropic spatial filter and (b) an anisotrpic filter, as compared with the truth in solid lines.*

OSSE and real data experiments are being performed that will examine the slant-path GPS data on the short range forecast of precipitation.

### *2.4 Ensemble Kalman filter data assimilation*

Ph.D. student, Mingjing Tong, who finished her Ph.D. degree in May 2006 and continued as a post-doc under partial support of this grant, developed an ensemble Kalman filter (EnKF) system based on the ARPS model and applied it to the assimilation of radar radial velocity and/or reflectivity data at the convective scale (Tong and Xue 2004, 2005; Tong 2006). Based on a set of OSS experiments, Tong and Xue (2005) show that not only can the wind and thermodynamic fields be retrieved accurately, but all five categories of hydrometeors employed by the ice microphysics scheme can also be successfully retrieved.

In Xue et al (2006), the ARPS EnKF data assimilation system is used to study the effectiveness and impact of data from a network of then-planned four low-cost radars for the Oklahoma test-bed of CASA. The benefit of having these radars providing low-level coverage missing from NEXRAD is clearly demonstrated. A new project involving EnKF is the assimilation of polarimetric Doppler radar data and initial results with simulated data are encouraging (Jung et al. 2006). Godfrey et al. (2005) applied the EnKF method to further study the impact of CASA radar data and scanning strategies on the analysis and prediction of storms of different types.

In Tong and Xue (2006a; 2006b), the EnKF method is for the first time applied to simultaneous estimation of the atmospheric state and parameters in an ice microphysics scheme. Fig. 6 shows the absolute ensemble mean errors of the four parameters (incept parameters for rain, snow and hail drop/particle size distributions and hail density) averaged over the 16 experiments using error-containing data (gray curves) and error-free data (black curves. In the error-containing case, the average absolute error of $n_{0r}$ decreases below 2 times the initial error standard deviation (SD) after 5 assimilation cycles and the error is reduced below one SD in the last 3 assimilation cycles. At the end of the assimilation cycles, the errors of $n_{0s}$, $n_{0h}$ and $\rho_h$ are all between 1 and 2 SD. Using the error-free data, the errors of the estimated parameters are significantly smaller; they are reduced below 1 SD for all four parameters at the end of the assimilation cycles.

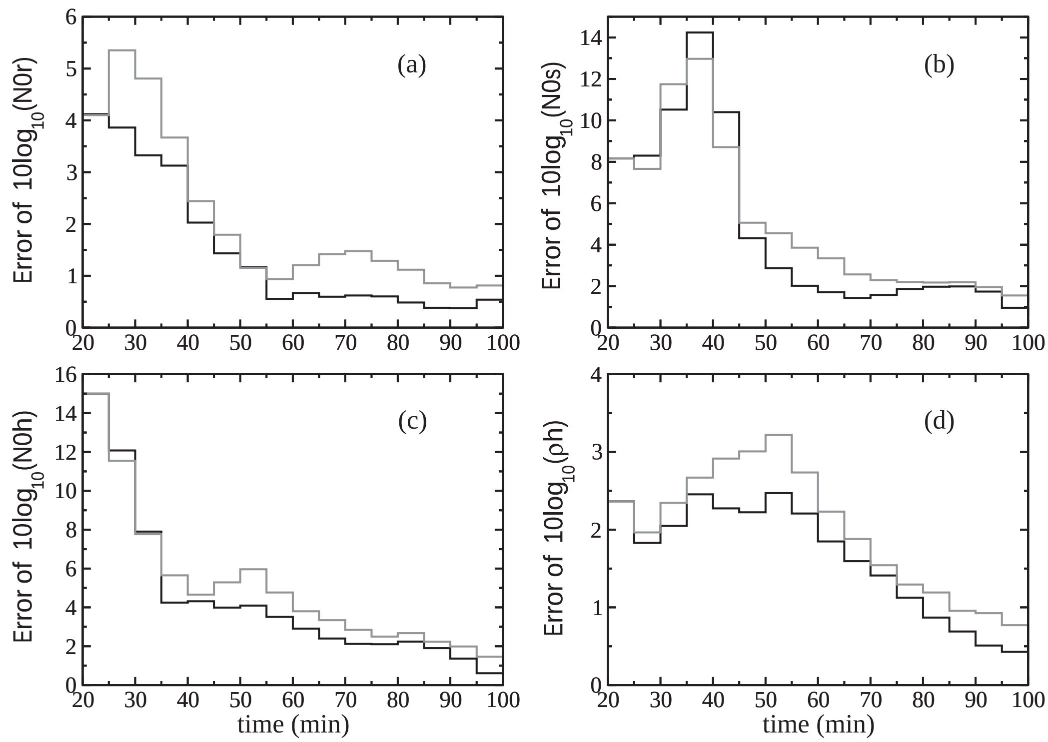


*Fig. 6. The evolution of the average ensemble-mean absolute error of $10log_{10}(n_{0r})$ (a), $10log_{10}(n_{0s})$ (b), $10log_{10}(n_{0h})$ (c), and $10log_{10}(\rho_h)$ (d), calculated from the 16 experiments simultaneously estimating rain intercept parameter $n_{0r}$, snow intercept parameter $n_{0s}$, hail intercept parameter $n_{0h}$, and hail density $\rho_h$ using error-containing reflectivity data (gray) and error-free reflectivity data (black).*

Studies with EnKF and real data are so far very limited. With real data, the presence of model error poses many more challenges not faced when assimilating simulated data using a perfect model. Within M. Tong's Ph.D. study (Tong 2006), she applied our EnKF system to the May 29-30, 2004 northern Oklahoma City tornado thunderstorm case. The radial velocity and reflectivity data from Oklahoma City WSR-88D (KTLX) and/or Enid, OK (KVNX) radars were assimilated. The assimilation used a 180x120 km grid at 1 km resolution, and 40 ensemble members. The results are rather encouraging. Fig. 7 shows the analyzed reflectivity at the end of a 1-hour assimilation period, interpolated to the 0.86º elevation of KTLX radar (left panel), as compared to the observation (right panel). The analyzed storm exhibits typical supercell structures, including low-level hook echo, mid-level mesocyclone, intense updraft, as well as low-level gust front and convergence center. Fig. 8 shows the results of analyzing two WSR-88D radars (KTLX and KVNX) for this case, using ARPS 3DVAR analysis as the initial guess instead of a single sounding, and using the full physics ARPS model in the assimilation cycles. The analyzed storm exhibits dynamically consistent structures include intense updraft located in the hook echo region, and mesocyclone circulations. Work continues in improving the general EnKF assimilation algorithms and evaluating the impacts of various sources of errors with this and other cases.

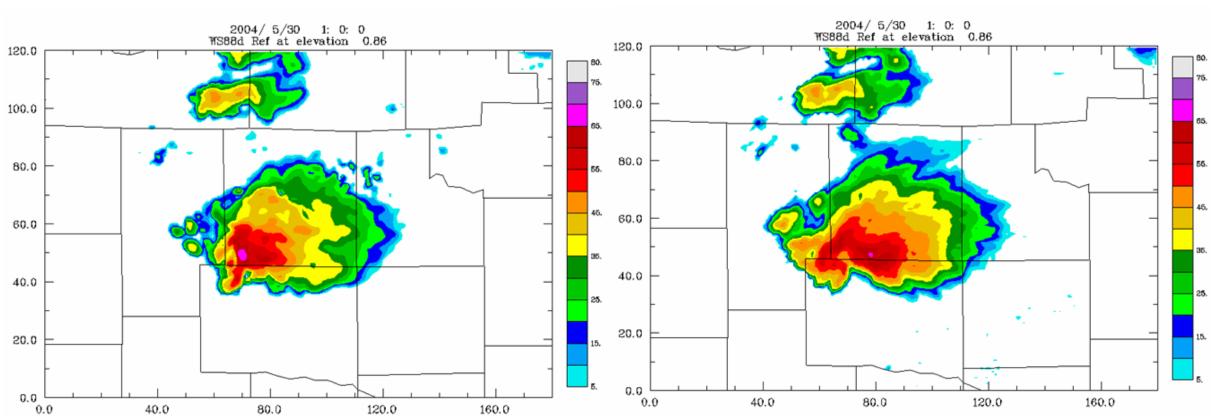

*Fig. 7. The analyzed reflectivity field at the 0.86º elevation (left) as compared to the corresponding observed reflectivity (right), at the end of a hour-long assimilation period, for the May 29-30 2004 north Oklahoma City tornadic thunderstorm. OKC WSR-88D radar radial velocity and reflectivity data were assimilated.*

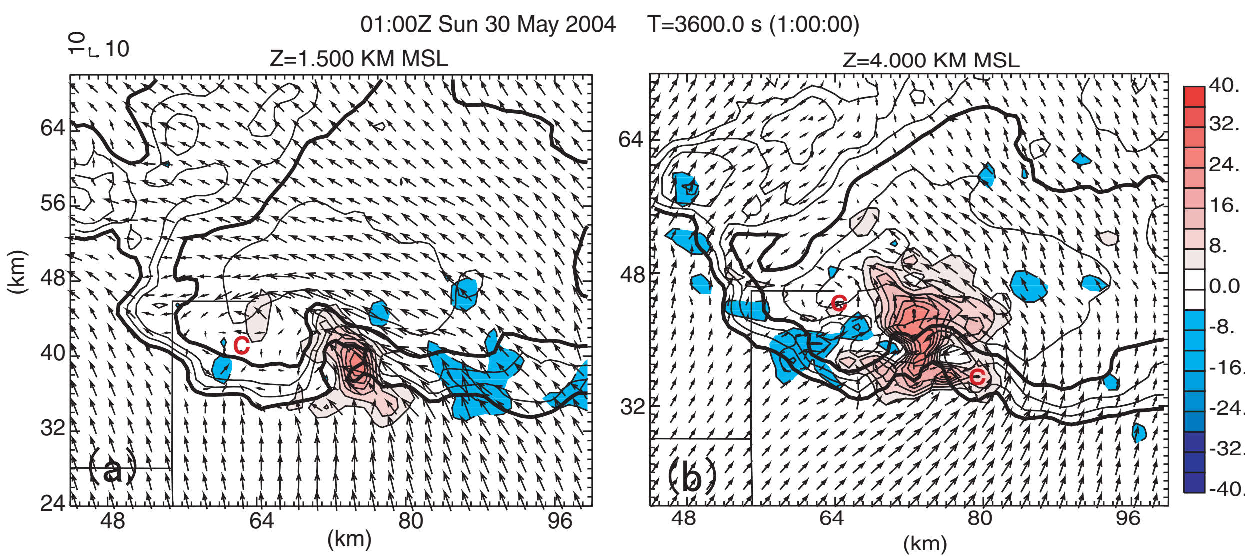


*Fig. 8. EnKF-analyzed vertical velocity [ contours and shading, solid (dash) contours represent positive (negative) w ] and horizontal storm-relative winds (vectors, plotted every other grid point) and reflectivity (contours at intervals of 10 dBZ starting from 10dBZ, with the 40 dBZ contours highlighted) at (a) 1.5 km MSL and (b) 4 km MSL at 0100 UTC 30 May from experiment assimilating both KTLX and KVNX radar data starting from inhomogeneous initial environmental conditions provided by 3DVAR analysis and the full model physics ARPS model. Radar data are assimilated every 5 minutes starting from 0000 UTC 30 May, 2004.*

Under the partial support of this grant, Gao and Xue (2006a; 2006b) developed an efficient dual-resolution EnKF data assimilation algorithm in which observations are assimilated on a single high-resolution grid using flow-dependent background error covariance estimated from a lower-resolution ensemble. It is shown that flow-dependent background error covariances estimated from the lower-resolution ensemble are effective in producing quality analyses from radar data at the high resolution; the system is able to reestablish the model storm fairly accurately after ten or so assimilation cycles. This method significantly reduces the computational cost of ensemble Kalman filter.

### *2.5 Data impact and convective initiation studies for IHOP cases*

The data impact study by Dawson and Xue (2006) further demonstrated the positive impact of cloud analysis using reflectivity data from multiple radars and the assimilation of other special sources of data (e.g., surface observations from over 10 regional mesonets) collected during the 2002 IHOP field campaign for the forecast of a mesoscale convective system (MCS). A significant positive impact, of cloud analysis in particular, was found to last for at least 12 hours in this case.

The convective initiation processes of the same 24 May 2002 case were studied in depth in two other IHOP special issue papers (Xue and Martin 2006a; 2006b), through high-resolution (1 km) numerical simulations using ARPS and ADAS. By assimilating high-density surface networks (e.g., the Texas Mesonet) and other special observations from IHOP, three series of convective cells initiated at specific locations of the dryline were accurately predicted to within 20 min and 25 km of the true cells. The model also correctly predicted the lack of initiation of convection at the dryline-cold front triple point to the north, on which a large array of instruments were focused on that day. The evolution of the simulated dryline and the convective initiation process were analyzed in great detail. For the first time, the exact process by which boundary-layer eddies and horizontal convective rolls interact with the dryline convergence line to determine the exact locations of cell initiation were simulated for a real case. Many simulated features at various scales were found to agree well with new (IHOP) and past observational data. Based on these simulations, a new conceptual model for dryline convective initiation was proposed.

In Xue and Martin (2006a), it is suggested that the interaction between the dryline and the horizontal convective rolls from the west side of the dryline play an important role in determining the preferred locations of convective initiation along the dryline. Such interaction creates surface convergence maxima that provide additional forcing to lift air parcels above their level of free convection (LFC). The mesoscale convergence in the dryline zone and the resultant upward bulging of the well-mixed moist boundary layer created a favorable zone for moist convection. In Xue and Martin (2006b), the development and evolution of the boundary layer (BL) horizontal convective rolls (HCRs), and open convective cells (OCCs) and their interaction with the dryline are analyzed in detail. The processes by which a series of (moist) convective cells are triggered and the possible role of misocyclone vortices that form along the main convergence line are analyzed in detail. A new conceptual model that summarizes our findings is proposed.

Data impact studies have also be performed for other IHOP case. New results for the 12-13 June 2002 IHOP convective initiation case are excellent and are summarized in Liu and Xue (2006b) and Xue and Liu (2006). Fig. 9 compares with radar observations the 6-hour ARPS forecast of convective cells initiated along a dryline and a thunderstorm outflow boundary, in which special data collected by IHOP were assimilated hourly over a 6-hour period. The 3 km and 1 km grids used had about 300x800 and 860x700 grid points in the horizontal, respectively.

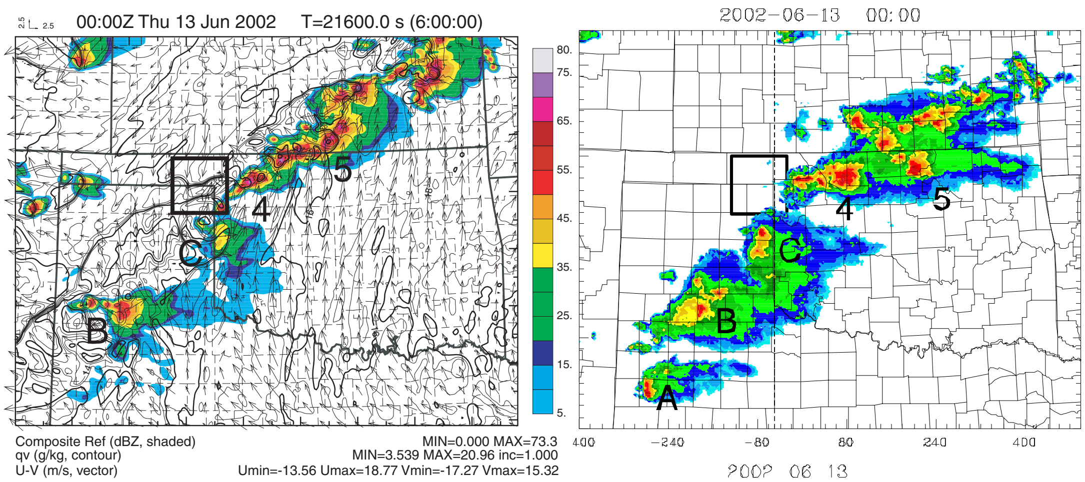


*Fig. 9. Left: The forecast surface water vapor mixing ratio (contours, g kg$^{-1}$), the wind vector (m s$^{-1}$) and composite reflectivity (shaded, dBZ) at 0000 UTC, 13 June, 2002. Right: The observed low-level reflectivity field valid at the same time. The capital letters and bold numbers indicate the locations of primary convective cells.*

### *2.6 Implementation of multi-moment microphysics scheme and sensitivity of QPF to microphysical parameterizations*

Leveraging on CAPS internal resources, the Milbrandt and Yau (2005a; 2005b, MY05 hereafter) multi-moment ice microphysics scheme was implemented inside the ARPS. The package contains single, double, triple moment options and a 2.5-moment option in which the shape parameter in the gamma distribution is diagnosed. In the triple moment case, the model predicts total number concentration (zero moment), mixing ratio (third moment) and reflectivity (sixth moment). A number of technical issues had to be resolved before the scheme produces reasonable solutions in the ARPS implementation. Further, the WRF single-moment six-category ice physics scheme (WSM6, Hong and Lim 2006) and its modified version that diagnoses intercept parameters from mixing ratios have also been implemented in the ARPS. These schemes provide us the capabilities to, among other things, examine the sensitivities of QPF to microphysics of different degrees of sophistication.

Graduate student Dan Dawson tested and debugged the initial implementation of the MY05 scheme. He applied the scheme to the May 3$^{rd}$, 1999 Oklahoma City tornado case, initializing the case using ADAS and ARPS cloud analysis package. Initial results on a 3-km grid are encouraging, though a number of known issues remain, including the consistency between the cloud analysis package with the multi-moment microphysics during the data assimilation cycles, which are being addressed in ongoing work.

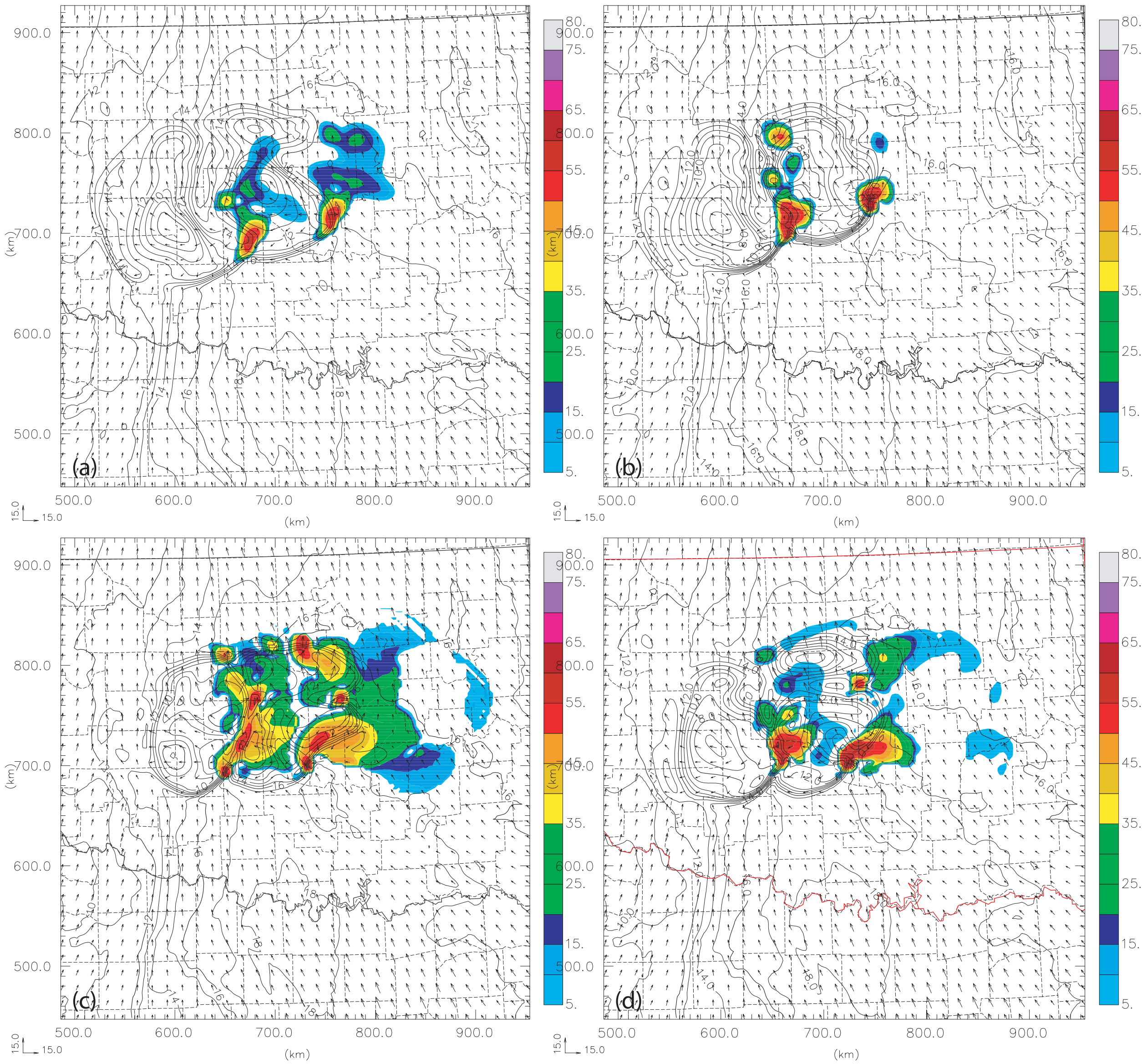

*Fig. 10. Simulated surface reflectivity and contours of water vapor mixing ratio (1 g/km increments) at 2 hrs (0000 UTC) into the 3 km forecast for a) ARPS Lin scheme, b) MY 1-moment scheme, c) MY 2-moment scheme, and d) MY 3-moment scheme.*

Fig. 10 compares the results of the May 3rd, 1999 Oklahoma City tornadic thunderstorm case at 0000 UTC, 2 hours into the prediction, using the ARPS default Lin et al. (1983) ice microphysics and MY05 single, double and triple moment schemes. It is seen that the Lin scheme and MY1 scheme results are very similar (Fig. 10a,b), with both exhibiting compact reflectivity cores with a stunted forward flank region in the two main right-moving supercells. These storms correspond to storms A and B from the observations (not shown). Predicting 2 or 3 moments in the microphysics scheme (Fig. 10 c,d) results in a much more realistic reflectivity structure, particularly in the forward flank region of the storms. On the other hand, all simulations exhibit strong and extensive surface cold pools, which were not observed, which affected the evolution and track of the storms, mainly by keeping the storms on a more east-northeasterly track, rather than the observed northeasterly track. Ongoing work involves running on higher resolution grids (1 km and higher) and examining the causes of the overly intense cold pools in the simulations.

## 3 Education and Training

This research grant provided support for 3 Ph.D. students (Mingjing Tong, Haixia Liu, Daniel Dawson) and two post-doctoral scientists (William Martin and Mingjing Tong). The primary stipend support of Dan Dawson came from his NSF Graduate Fellowship and Mingjing Tong completed her Ph.D. degree in May 2006 and continued within this project as a post-doc at 50% FTE. All four of them were supported by our previous NSF grant, ATM-0129892. This grant also provided up to one month of support for the PIs.

## 4 Thesis and Dissertation Completed

Tong, M., 2006: Ensemble Kalman filer assimilation of Doppler radar data for the initialization and prediction of convective storms, Ph.D. Dissertation, School of Meteorology, University of Oklahoma, 243 pp.

## 5 References cited, with those completed under complete or partial support of this grant proceeded with a '*'

*Dawson, D. T., II and M. Xue, 2006: Numerical forecasts of the 15-16 June 2002 Southern Plains severe MCS: Impact of mesoscale data and cloud analysis. *Mon. Wea. Rev.*, **134,** 1607-1629.

*Gao, J. and M. Xue, 2006a: An efficient dual-resolution approach for ensemble data assimilation and tests with the assimilation of Doppler radar data. *Mon. Wea. Rev.***,** To be submitted.

*Gao, J. and M. Xue, 2006b: An efficient dual-resolution ensemble data assimilation approach and tests with the assimilation of Doppler radar data. Extended abstract, 10th Symposium on Integrated Observing and Assimilation Systems for the Atmosphere, Oceans and Land Surface (IOAS-AOLS),, Atlanta, GA, Amer. Meteor. Soc.,.

*Gao, J., K. Brewster, and M. Xue, 2006a: A comparison of the radar ray path equations and approximations for use in radar data assimilation. *Adv. Atmos. Sci.*, **23,** 190-198.

*Gao, J., K. Brewster, and M. Xue, 2006b: Sensitivity of radio refractivity to moisture and temperature and its influence on radar ray path. *J. Appl. Meteor. Climatol.***,** Submitted.

*Gao, J., M. Xue, S. Y. Lee, K. K. Droegemeier, and A. Shapiro, 2006c: A three-dimensional variational method for velocity retrievals from single-Doppler radar observations on supercell storms. *Meteo. Atmos. Phys.***,** DOI 10.1007/s00703-005-0170-7.

*Godfrey, E. S., M. Tong, M. Xue, and K. K. Droegemeier, 2005: Assimilation of simulated network radar data of veried storm types using EnSRF for convective storm analysis and forecasts. Extended abstract, 17th Conf. Num. Wea. Pred., Washingtong DC, Amer. Meteor. Soc., 13A.1.

Hong, S.-y. and J.-O. J. Lim, 2006: The WRF single-moment 6-class microphysics scheme (WSM6). *J. Korean Meteor. Soc.*, **42,** 129-151.

*Hu, M., 2005: 3DVAR and cloud analysis with WSR-88D level-II data for the prediction of tornadic thunderstorms, Ph. D. Dissertation, School of Meteorology, University of Oklahoma, 217 pp.

*Hu, M. and M. Xue, 2006: Impact of configurations of rapid intermittent assimilation of WSR-88D radar data for the 8 May 2003 Oklahoma City tornadic thunderstorm case. *Mon. Wea. Rev.***,** Accepted.

*Hu, M., M. Xue, and K. Brewster, 2006a: 3DVAR and cloud analysis with WSR-88D level-II data for the prediction of Fort Worth tornadic thunderstorms. Part I:  Cloud analysis and its impact. *Mon. Wea. Rev.*, **134,** 675-698.

*Hu, M., M. Xue, J. Gao, and K. Brewster, 2006b: 3DVAR and cloud analysis with WSR-88D level-II data for the prediction of Fort Worth tornadic thunderstorms. Part II:  Impact of radial velocity analysis via 3DVAR. *Mon. Wea. Rev.*, **134,** 699-721.

*Jung, Y., M. Xue, G. Zhang, and J. Straka, 2006: Assimilation of polarimetric radar data using ensemble Kalman filter: Direct assimilation with simulated data. *Mon. Wea. Rev.***,** To be submitted.

Lin, Y.-L., R. D. Farley, and H. D. Orville, 1983: Bulk parameterization of the snow field in a cloud model. *J. Climate Appl. Meteor.*, **22,** 1065-1092.

*Liu, H. and M. Xue, 2006a: Retrieval of moisture from slant-path water vapor observations of a hypothetical GPS network using a three-dimensional variational scheme with anisotropic background error. *Mon. Wea. Rev.*, **134,** 933–949.

*Liu, H. and M. Xue, 2006b: Prediction of convective initiation and storm evolution on 12 June 2002 during IHOP. Part I: Control simulation and sensitivity experiments. *Mon. Wea. Rev.***,** To be submitted.

*Liu, H., M. Xue, R. J. Purser, and D. F. Parrish, 2006: Retrieval of moisture from simulated GPS slant-path water vapor observations using 3DVAR with anisotropic recursive filters. *Mon. Wea. Rev.***,** In press.

*Martin, W. J. and M. Xue, 2006a: Initial condition sensitivity analysis of a mesoscale forecast using very-large ensembles. *Mon. Wea. Rev.*, **134,** 192–207.

*Martin, W. J. and M. Xue, 2006b: Evolved and random perturbation methods for calculating model sensitivities and covariances. *Mon. Wea. Rev.***,** To be submitted.

*Martin, W. J. and M. Xue, 2006c: Determining sensitivities, impacts and covariances from very large ensembles with randomly perturbed initial conditions. *Mon. Wea. Rev.***,** To be submitted.

Milbrandt, J. A. and M. K. Yau, 2005a: A multi-moment bulk microphysics parameterization. Part I: Aanlysis of the role of the spectral shape parameter. *J. Atmos. Sci.*, **62,** 3051-3064.

Milbrandt, J. A. and M. K. Yau, 2005b: A multi-moment bulk microphysics parameterization. Part II: A proposed three-moment clousre and scheme description. *J. Atmos. Sci.*, **62,** 3065-3081.

*Tong, M., 2006: Ensemble Kalman filer assimilation of Doppler radar data for the initialization and prediction of convective storms, Ph.D. Dissertation, School of Meteorology, University of Oklahoma, 243 pp.

*Tong, M. and M. Xue, 2004: Ensemble Kalman filter assimilation of Doppler radar data with a compressible nonhydrostatic model. Extended Abstract, 20th Conf. Wea. Analy. Forecasting/16th Conf. Num. Wea. Pred., Seattle, WA, Amer. Meteor. Soc.

*Tong, M. and M. Xue, 2005: Ensemble Kalman filter assimilation of Doppler radar data with a compressible nonhydrostatic model: OSS Experiments. *Mon. Wea. Rev.*, **133,** 1789-1807.
*Tong, M. and M. Xue, 2006a: Simultaneous estimation of microphysical parameters and atmospheric state with radar data and ensemble square-root Kalman filter. Part I: Sensitivity analysis and parameter identifiability *Mon. Wea. Rev.***,** Under review.
*Tong, M. and M. Xue, 2006b: Simultaneous estimation of microphysical parameters and atmospheric state with radar data and ensemble square-root Kalman filter. Part II: Parameter estimation experiments. *Mon. Wea. Rev.***,** Under review.
*Xue, M. and W. J. Martin, 2006a: A high-resolution modeling study of the 24 May 2002 case during IHOP. Part I: Numerical simulation and general evolution of the dryline and convection. *Mon. Wea. Rev.*, **134,** 149–171.
*Xue, M. and W. J. Martin, 2006b: A high-resolution modeling study of the 24 May 2002 case during IHOP. Part II: Horizontal convective rolls and convective initiation. *Mon. Wea. Rev.*, **134,** 172–191.
*Xue, M. and H. Liu, 2006: Prediction of convective initiation and storm evolution on 12 June 2002 during IHOP. Part II: High-resolution simulation and mechanisms of convective initiation**,** To be submitted.
*Xue, M., M. Tong, and K. K. Droegemeier, 2006: An OSSE framework based on the ensemble square-root Kalman filter for evaluating impact of data from radar networks on thunderstorm analysis and forecast. *J. Atmos. Ocean Tech.*, **23,** 46–66.